

Pectoral muscle segmentation on mammographic images based on radial lengths

Sevastianos Chatzistergos, *Member, IEEE*, Ioannis Andreadis, *Member, IEEE*,
and Konstantina S. Nikita, *Senior Member, IEEE*

Abstract—Mammography is the main imaging technique for breast cancer diagnosis and prevention. Many image processing techniques though require the breast region to be adequately defined in order to provide reliable results. Pectoral muscle segmentation is one of the most challenging tasks in this domain since the limits between the muscle and the actual breast region are sometimes quite difficult to distinguish. In the current work, a method to perform pectoral muscle segmentation on mammographic images based on the notion of Radial Lengths (*RL*) is presented. The mean value of *RLs* is used to reveal edge regions in mammograms. The edges produced would be discontinued and resemble mostly to edge segments. Points at those segments are then randomly selected and candidate edge lines start propagating having those points as a start. A number of criteria are set to define how well the line follows the actual muscle edge. A single line representing the pectoral muscle edge is finally selected based on a number of fitting criteria. The proposed method is compared to state of the art methods in the field and found to clearly outperform them.

Index Terms—pectoral muscle, segmentation, breast, mammogram.

I. INTRODUCTION

MAMMOGRAPHY is the main imaging technique to screen women for the detection and diagnosis of breast cancer. But reading mammograms is known to be a very demanding job for radiologists, since judgments depend on training, experience, and subjective criteria [1]. To this end, Computer Aided Diagnosis (*CAD*) system can provide invaluable help not only in alleviating radiologists by automatically performing certain tasks but also provide a second opinion that is generally considered objective. Things get complicated though when pectoral muscle is present on the mammogram. The success of CAD systems depend on an accurate differentiation between the pectoral muscle and breast tissue mass [2]. There are number of reasons why this happens, but the main reason is that it reduces the search area for abnormalities and makes it limited to the relevant region of the breast without excessive influence from the background of the mammogram, which typically includes annotations and artifacts that could have an adverse effect on the analysis [3]. On the other hand though, segmentation of the pectoral muscle has been proven to be quite tricky since delineation between the pectoral muscle and breast tissue is not evident in most cases [4], [5].

Various methods have been proposed in the literature to define and segment the pectoral muscle. Kwok et al. [6] used

Hough transform to receive a straight line estimation of the pectoral muscle and then refine the estimation using iterative "cliff detection". One disadvantage of the method is its weakness to detect edges between different textures since intensity edges in many cases are replaced by fuzzy texture edges on the pectoral boundary. Ferrari et al. [7] suggested the use of a number of specially designed gabor filters to enhance the pectoral muscle edge. The image is convolved with the gabor filters and using vector-summation, a magnitude and a phase image are generated. The magnitude value of each image pixel is propagated along the phase direction and the resulting image is used to detect candidate pectoral muscle edges. A post processing step is then used to find the true muscle edge. One disadvantage of the method though is that when the glandular tissue obscures the pectoral muscle, the segmented pectoral muscle may be underestimated [8]. Ma et al. [9] presented a method based on adaptive pyramids and an other one based on minimum spanning trees. The two methods did not perform well when strong lined were present inside and parallel to the actual muscle border. Li et al. [8] used anatomical features of the pectoral muscle homogeneous texture and high intensity deviation to define an initial pectoral muscle edge, Liu et al. [10] combined the iterative Otsu thresholding scheme and the mathematic morphological processing to find a rough border of the pectoral muscle. The multiple regression analysis (MRA) was then employed on the rough border to obtain an accurate segmentation of the pectoral muscle. Mustra et al. [11] presented a pectoral muscle detection method based on a combination of contrast enhancement using adaptive histogram equalization and polynomial curvature estimation on selected region of interest. Hong et al. [12] proposed a topographic representation called the isocontour map, in which a salient region forms a dense quasi-concentric pattern of contours to segment various breast regions including pectoral muscle.

In the current work a method to perform pectoral muscle segmentation based on Radial Lengths is presented [13]. Radial Lengths are used to first define a number of candidate muscle edge points and then provide guidance in a line propagation process. The paper is organized as follows: Section II presents Radial Lengths, while the actual pectoral muscle determination method is given in section III. Section IV contains information about the dataset used, while results and conclusion are given in sections V and VI.

II. RADIAL LENGTHS

In our previous work [13] we demonstrated the ability to reveal diagnostically critical information in mammograms

S. Chatzistergos is with the Department of Electrical and Computer Engineering, National Technical University of Athens, Greece, e-mail: schatzist@biosim.ntua.gr .

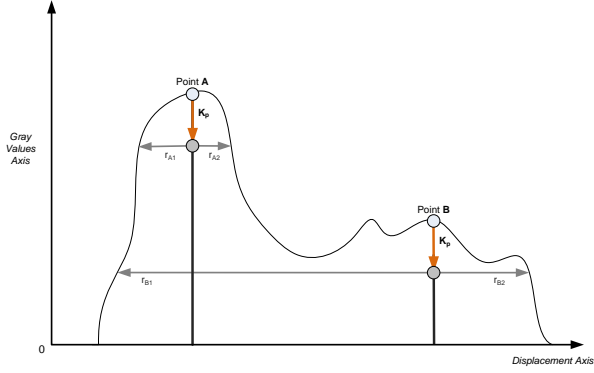


Fig. 1. Demonstration of Radial Lengths Method on an image slice. Radial lines start propagating at every image point after a value K_P is subtracted from the image gray value at the corresponding point. Propagation will stop if the image boundaries are met. Points belonging to high density regions (Point A) will present smaller radial length values (r_{A1}, r_{A2}), while points belonging to fat tissue regions (Point B) will present larger radial length values (r_{B1}, r_{B2}).

using a series of equally rotated radials that propagate until they meet a certain limit. In this work we propose again the use of radial lengths in the process of pectoral muscle segmentation in a modified manner though.

The original concept was to consider the mammographic image as a three dimensional shape where the image gray value at a certain point (x_0, y_0) defined the z -axis value of the shape boundary. Given an image point (x_0, y_0) and therefore an image gray value $I(x_0, y_0)$ at that point, if a certain value K_P is subtracted from $I(x_0, y_0)$, it would be like moving inside the interior of the three dimensional shape. Then a line starting from (x_0, y_0) at a given angle in relation to axis x but remaining always parallel to the surface defined by axes x, y , could begin propagating until the shape boundary is found. The final length of the propagated line is termed Radial Length (RL). If a point (x_0, y_0) is located in a dense breast region would present a high gray value and therefore the relating lines would have smaller lengths (Fig. 1, Point A) in relation to fat tissue regions which present lower gray values (Fig. 1, Point B). For each image point, a fixed number of equally rotated lines were considered providing an equal number of radial lengths (r_i), the mean value of which is used to form I_{RL}

$$I_{RL}^{(x_0, y_0)} = \frac{\sum_{i=1}^N r_i^{(x_0, y_0)}}{N}, \quad (1)$$

where N is the total number of radial lengths r_i calculated around point (x_0, y_0) .

One important parameter is the selection of the appropriate rotation angle between two adjacent radial lines. Since these lines are equally rotated, angle selection comes down to total number of lines selection problem. In general a larger number of lines provides better results with higher computational cost. In our experiments we used a total number of 32 lines. Furthermore, pectoral muscle edge is generally expected to

have a certain orientation. Edge's angle in relation to the image coordinate system is expected to vary between $(-\frac{3\pi}{4}, 0)$. Since radial lines that meet the pectoral edge perpendicular are more effective in describing its location, only lines with angles between $(\frac{\pi}{4}, \frac{\pi}{2})$ are selected. Six radial lines present the appropriate orientation and therefore used in the determination of I_{RL} .

Parameter K_P at each image point is calculated using (2) on a local window W_i with length W^L , centered at the specific point.

$$K_P = a \cdot (\max(W_i) - \min(W_i)), \quad (2)$$

where a is user defined that takes values in $(0, 1)$ and $\max(W_i)$ and $\min(W_i)$ refer to the maximum and minimum gray value inside the window W_i , respectively. In our experiments $a = 0.15$ and $W^L = 20$.

III. PECTORAL MUSCLE EDGE DETERMINATION

In this section the actual process of pectoral muscle segmentation is presented. The main steps of the algorithm are the following: At first all images are sub sampled so as to become 256×256 and mirrored if necessary so that the pectoral muscle occupy the upper left region of the image. On each image I (1) is used to produce I_{RL} . I_{RL} then is used to determine a number of candidate pectoral muscle edge points from which lines (L_i), representing the edge between the muscle and the image, start propagating using I_{RL} as a guide. For each L_i a number of characteristics is calculated and if their values fall within predefined limits these lines are considered as candidate muscle edge lines ($Line_i^{Cand}$). A final selection between all $Line_i^{Cand}$ is then performed in order to define the best fitting pectoral muscle edge.

A. Candidate edge points

The determination of the appropriate candidate edge points is of great importance for the overall success of the algorithm since performance and speed depend largely on it. Although the algorithm can provide adequate results even if just a few actual muscle edge points are determined, in general the larger the number of candidate points that truly belong to the muscle edge the more liable and fast the final result.

In order to define the candidate edge points (I^{Cand}), I_{RL} is first smoothed using an averaging filter with size 2×2 pixels and then, the relative horizontal differences (I_{RL}^{diff}) are calculated

$$I_{RL}^{diff}(x_i, y_i) = \frac{I_{RL}(x_i, y_i) - I_{RL}(x_i, y_i - 1)}{I_{RL}(x_i, y_i)}. \quad (3)$$

A threshold ($T_C = 0.5$) is then applied to I_{RL}^{diff} to convert it into binary format. All 8-connected regions are defined and regions with less than 20 members are rejected.

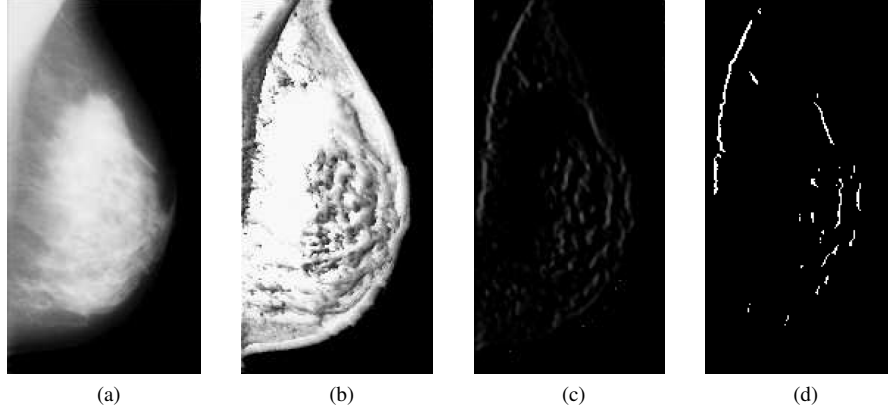


Fig. 2. Candidate pectoral muscle edge points selection. (a) Original image, (b) I_{RL} , (c) I_{RL}^{diff} , (d) Candidate edge points (I^{Cand}).

B. Candidate edge lines

From the candidate edge points, a number of lines is produced by propagation.

Before continuing with the propagation, an image (I_{Guid}) that will be used as a guidance during the propagation process needs to be defined

$$I_{Guid}(x_i, y_i) = \begin{cases} 100 & \text{if } I_{Mask}(x_i, y_i) = 0, \\ 0.01 \cdot I_{RL}(x_i, y_i) & \text{if } I_{RL}^{diff}(x_i, y_i) > T_C, \\ I_{RL}(x_i, y_i) & \text{else,} \end{cases} \quad (4)$$

where I_{Mask} is a mask image referring to the actual breast region. It is defined via a three class segmentation process on the original image gray levels, using k-means algorithm. I_{Mask} is comprised of all points belonging to the two teams with the larger mean values.

Therefore, I_{Guid} presents a very high value at locations outside the breast region, very low values at candidate edge points locations and values defined by I_{RL} at all other locations.

Fig. 2 presents the process described so far on image *mdb003*. More specifically, the original image (Fig. 2-a), I_{RL} (Fig. 2-b), I_{RL}^{diff} (Fig. 2-c) and I^{Cand} (Fig. 2-d) are provided.

C. Line propagation

At first, a single point is randomly selected (x_0, y_0) from all the candidate edge points and a line starts propagating. The propagation is firstly done upwards and then downwards.

During the propagation process, the orientation ($Angl_{Prop}$) of the propagating line near its growing end will need to be defined. In order to define that, a circle (C_{or}) is centered at the line's ending point (x_e, y_e) and the intersection point (x_i, y_i) between the line and circle is defined (Fig. 3). Then, $Angl_{Prop}$ is given by

$$Angl_{Prop} = \begin{cases} \arctan\left(\frac{y_e - y_i}{x_e - x_i}\right) & \text{if upward propagation,} \\ \arctan\left(\frac{y_i - y_e}{x_i - x_e}\right) & \text{if downward propagation.} \end{cases} \quad (5)$$

A special care needs to be taken for the calculation of $Angl_{Prop}$ when the first propagation step from the initial

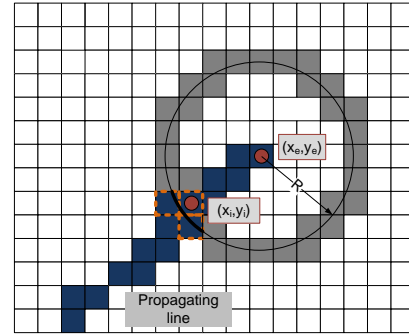


Fig. 3. Orientation determination near the ending point (x_e, y_e) of an upward propagating line using a circle with radius R centered at (x_e, y_e).

point (x_0, y_0) is attempted. More specifically, from I^{Cand} the 8-connected region to which (x_0, y_0) belongs, is specified. A circle C_{or} is then centered at (x_0, y_0) and $Angl_{Prop}$ is calculated using (5), where (x_e, y_e) = (x_0, y_0) and (x_i, y_i) are the coordinates of the lower intersecting point between the 8-connected region and C_{or} . We use the lower intersecting point since the line is propagating upwards at this step.

The basic concern during the propagation process from an initial point (x_e, y_e), is to find an appropriate image point (x_P, y_P) in the neighborhood of the initial (x_e, y_e) that fulfills a number of criteria and draw a line that connects them. The propagation continues considering (x_P, y_P) as the new initial point (x_e, y_e) and look for a new appropriate point (x_P, y_P) in it's neighborhood. Something that needs to be defined is the actual point neighborhood. Given the $Angl_{Prop}$ value of the propagating line segment, a number of rotated radials (q_j) is considered. These radials have their starting points at (x_e, y_e), their length is R and they are distributed around a central radial whose orientation matches the orientation of the initial line.

The radials' ending points define the requested neighborhood (N_P) (Fig. 4). A smaller value for R produces smoother propagating lines but with larger computational cost. In our case R is set equal to 5 pixels. The number of the radials used did not seem to affect significantly the final result.

In our experiments we used 9 radials and the radial angles used in relation to the initial line orientation are

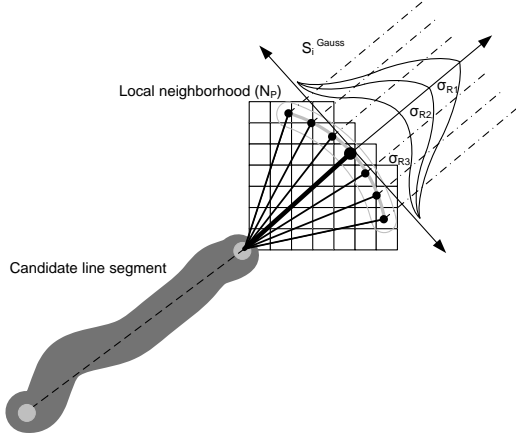


Fig. 4. Next point selection during line propagation. The selection is performed between points in local neighborhood N_P defined by radials emerging from line edge with length R at various angles in relation to line orientation. The next point is selected by combining the values of a guidance image at N_P points with Gaussian curves (S_j^{Gauss}) whose variance values (σ_R) are randomly selected.

$$\left\{-\frac{\pi}{6}, -\frac{\pi}{9}, -\frac{\pi}{12}, -\frac{\pi}{20}, 0, \frac{\pi}{20}, \frac{\pi}{12}, \frac{\pi}{9}, \frac{\pi}{6}\right\}.$$

In order to select the appropriate neighborhood point for the propagation process a scaling factor based on a Gaussian curve (S_{gauss}) is used

$$S_j^{gauss} = e^{-\left(\frac{j-j_C}{\sigma_R}\right)^2}, \quad (6)$$

where j is the index of each radial and j_C is the index of the central radial which in our case is 5. Also, $\sigma_R = 4 \cdot j_T \cdot A_{rand}$, where A_{rand} is a randomly selected number between 0 and 1 and j_T the total number of radials. A new A_{rand} value is calculated every time a new neighborhood region is determined.

The radial j for which

$$F_j = \left(\frac{1}{1 + S_j^{gauss}}\right) I_{Guid}(x_j, y_j) \quad (7)$$

is minimized, is selected and therefore its ending points (x_j, y_j) become the new (x_P, y_P) points of the propagating line.

D. Line elimination

The procedure described so far will produce a number of candidate pectoral muscle edge lines ($Line_i^C$), therefore there is a need to define how well the candidate lines follow the muscle edge. In order to accomplish that, two measures are performed.

The first measure is the average value (V_i) of I_{Guid} using only the points of $Line_i^{Cand}$ and is calculated using

$$V_i = \frac{1}{N_V} \sum_{x=1}^N \sum_{y=1}^M (I_{Guid}(x, y) \cdot \delta(Line_i^{Cand}(x, y))), \quad (8)$$

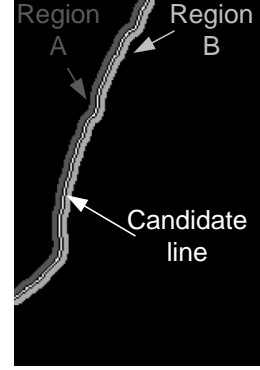


Fig. 5. Candidate pectoral muscle edge line (candidate line) and relating $Region_A$ and $Region_B$. $Region_A$ would typically be part of the pectoral muscle region, while $Region_B$ would typical be part of the actual breast region.

where

$$N_V = \sum_{x=1}^N \sum_{y=1}^M (\delta(Line_i^{Cand}(x, y)))$$

and $\delta(x)$ is delta Dirac.

Small values of V_i indicate that $Line_i^{Cand}$ follows a path that is very close to a strong edge. If V_i is larger than a threshold ($V^{Thres} = 2.5$) $Line_i^{Cand}$ is rejected. But strong edges could also be found at the border between breast region and the background.

Therefore, a second measure to eliminate those lines is required. This measure is based on the difference of the mean values (S_i) between two regions of the original image I , defined perpendicular to $Line_i^{Cand}$. The two regions are defined by performing a morphological dilation on the candidate line with a disk shaped structural element with radius $D_{rad}=5$ pixels and then subtracting the original line. This operation provides two distinct regions. The region closer to the left image side should ideally belong to the muscle region ($Region_i^A$) while the other should ideally belong to the breast region ($Region_i^B$) (Fig. 5).

$$S_i = S_i^A - S_i^B, \quad (9)$$

where

$$S_i^A = \frac{1}{N_A} \sum_x \sum_y (I(x, y) \cdot \delta(Region_i^A(x, y))), \quad (10)$$

$$S_i^B = \frac{1}{N_B} \sum_x \sum_y (I(x, y) \cdot \delta(Region_i^B(x, y))) \quad (11)$$

and

$$N_B = \sum_x \sum_y (\delta(Region_i^B(x, y))),$$

$$N_A = \sum_x \sum_y (\delta(Region_i^A(x, y))).$$

Large values of the S_i measure indicate that $Region_i^A$ and $Region_i^B$ differ significantly and therefore that $Line_i^{Cand}$ provides a satisfactory segmentation of the pectoral muscle.

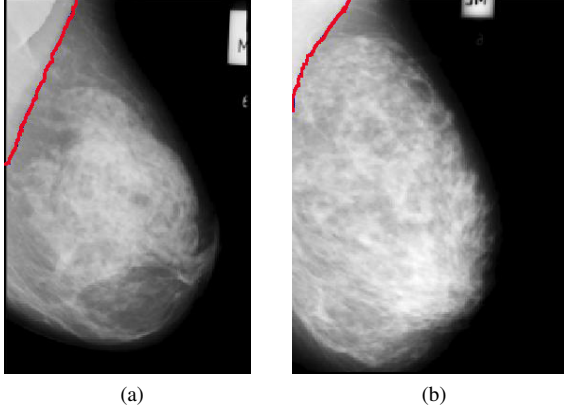


Fig. 6. Pectoral muscle segmentation results on mammogram images using the proposed method on (a) *mdb125* and (b) *mdb130*.

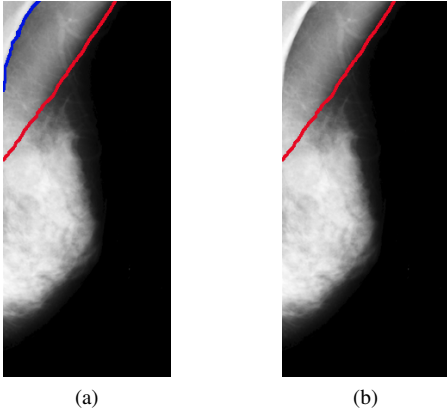


Fig. 7. Image with axillary folds (*mdb040*). (a) Candidate pectoral muscle edges. (b) Pectoral muscle segmentation result using proposed method.

If S_i is smaller than a certain threshold ($S^{Thres} = 10$), $Line_i^{Cand}$ is rejected. This would generally be the case for lines following the breast region border.

E. Final line selection

An adequate number of candidate lines that fulfill the criteria set, needs to be defined in order to increase the possibility of efficient pectoral muscle identification. Therefore, the line determination procedure is repeated selecting different initial point each time. The maximum number of repetitions is set to three times the number of candidate edge points, while the repetition will stop if the number of lines become greater than 50. The $Line_i^{Cand}$ with the smaller V_i value is selected. Fig. 6 shows two images segmented using the proposed method.

There are many cases though, where two edges are present within the muscle region (Fig. 7). This would commonly happen if axillary folds are present during the mammogram procedure. In those cases, the algorithm will have to be able to identify the existence of multiple edges and keep those $Line_i^{Cand}$ that present larger area values (E_i^{Line}). E_i^{Line} is defined as the area between the given edge and the upper left point of the image.

To accomplish that, E_i^{Line} values from all the remaining $Line_i^{Cand}$ are calculated and given as input to a k-means

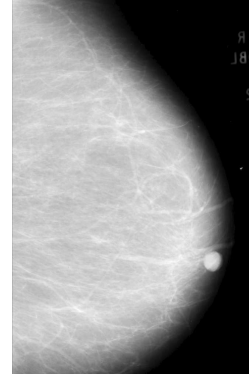


Fig. 8. Image *mdb098*. The proposed algorithm failed to define any pectoral muscle edge.

clustering algorithm that performs a partitioning into two sets. If the mean area values of $Line_i^{Cand}$ on each set differ significantly, then all $Line_i^{Cand}$ that belong to the set with the smaller area values are rejected. The two sets are considered to differ significantly if the mean value of the smaller area set is less than half the mean value of the set with the larger mean value.

Again, the $Line_i^{Cand}$ with the smaller V_i value is selected.

IV. DATASET

In order to perform the evaluation of the proposed method images from the mini-Mias database are used. These images are 1024×1024 pixels with $200\mu\text{m}/\text{pixel}$. The database consists of 322 images from 161 patients with odd numbered ones representing right mammogram and even numbered ones representing the left. From those images a subset with 84 images is constructed. The subset contains the same images as the ones used in [7] in order to provide results that can easily be compared and evaluated.

V. RESULTS

The proposed method is evaluated using the normalized area error [7] between the defined pectoral muscle edge and a corresponding hand-drawn edge image provided by [7]. The normalized area error consists of two parameters, the false positive pixels parameter (FP_i) and the false negative pixels parameter (FN_i). FP_i is the number of pixels that are identified falsely as belonging to the pectoral muscle region divided by the total number of pixels that really belong to the muscle area (N_{TT}). FN_i on the other hand is the number of pixels that are falsely identified as not belonging to the muscle region divided again by the total number of pixels that really belong to the muscle area.

It should be noted that from the 84 images, there is one case (*mdb098*) where our method failed to define any pectoral muscle edge. This image is given at Fig. 8. It can be seen though, that the muscle region is quite small and subtle.

The performance of the proposed algorithm in comparison with a number of state-of-the-art methods is given in table I. It can be seen that the proposed method provides the lowest value among all other methods as regards the FN value. On

TABLE I
SEGMENTATION PERFORMANCE ANALYSIS BY NORMALIZED AREA ERROR

	Gabor [7]	AP [9]	ID [8]	Proposed
FP	0.0058	0.0371	0.0145	0.0197
FN	0.0577	0.0595	0.0552	0.0471
$FP < 0.05$ & $FN < 0.05$	45	50	48	57
$\min(FP, FN) < 0.05$ & $0.05 < \max(FP, FN) < 0.10$	0	18	28	17
$\min(FP, FN) < 0.05$ & $\max(FP, FN) < 0.10$	0	11	7	7
$0.05 < FP < 0.10$ & $0.05 < FN < 0.10$	22	0	0	1
$0.05 < \min(FP, FN) < 0.10$ & $\max(FP, FN) > 0.10$	0	0	1	1
$FP > 0.10$ & $FN > 0.10$	17	5	0	0

the other hand, FP value of the proposed method is larger than Gabor and ID method. However, if the distribution of results to the various error range categories is considered, the proposed method outperforms all others. More specifically, 57 (about 69%) of cases belong to the lowest error range category for the proposed method, as compared to 48 (about 57%) for ID , 50 for AP (about 60%) and 45 (about 54%) for Gabor method. Furthermore, as far as the Gabor method is concerned, 17 cases (about 20%) belong to the highest error range category which is the largest value among all comparing methods for the particular category.

VI. CONCLUSION

A method to perform pectoral muscle segmentation on mammograms is presented. The method is based on Radial Lengths to provide an initial estimation of the muscle edge points and then perform a line propagation process from each such point. A number of fitting criteria are defined in order to define which of the propagated lines is the best estimation of the muscle edge and reject all others. The method is performed on specific 84 images from the *miniMias* dataset for which a hand-drawn pectoral muscle edge is available. Results indicate that the proposed method can effectively segment pectoral muscle providing comparable and in some aspects improved performance in comparison to the main methods in the field. Future work include the evaluation of the method on larger datasets and also the use of more evaluation criteria.

REFERENCES

- [1] H. D. Cheng, X. J. Shi, R. Min, L. M. Hu, X. P. Cai, and H. N. Du, "Approaches for automated detection and classification of masses in mammograms," *Pattern Recognition*, vol. 39, no. 4, pp. 646–668, 2006. [Online]. Available: <http://www.sciencedirect.com/science/article/pii/S0031320305002955>
- [2] S. Ciatto, M. Del Turco, G. Risso, S. Catarzi, R. Bonardi, V. Viterbo, P. Gnutti, B. Guglielmoni, L. Pinelli, A. Pandiscia, F. Navarra, A. Lauria, R. Palmiero, and P. Indovina, "Comparison of standard reading and computer aided detection (cad) on a national proficiency test of screening mammography," *European Journal of Radiology*, vol. 45, no. 2, pp. 135–138, 2003, cited By (since 1996)54. [Online]. Available: <http://www.scopus.com/inward/record.url?eid=2-s2.0-0037300318&partnerID=40&md5=4ed384bb479d26950a6b78d6c8bffe6e>
- [3] T. Majeed, N. Al-Jawad, and H. Sellahewa, "Breast border extraction and pectoral muscle removal in MLo mammogram images," in *Computer Science and Electronic Engineering Conference (CEECE), 2013 5th*, 2013, pp. 119–124.
- [4] L. Vincent and P. Soille, "Watersheds in digital spaces: An efficient algorithm based on immersion simulations," *IEEE Transactions on Pattern Analysis and Machine Intelligence*, vol. 13, no. 6, pp. 583–598, 1991, cited By (since 1996)2397. [Online]. Available: <http://www.scopus.com/inward/record.url?eid=2-s2.0-0026172104&partnerID=40&md5=a5b85a90d76a624b01bf45f417e2c742>
- [5] K. Ganesan, U. R. Acharya, K. C. Chua, L. C. Min, and K. T. Abraham, "Pectoral muscle segmentation: A review," *Computer Methods and Programs in Biomedicine*, vol. 110, no. 1, pp. 48–57, 2013. [Online]. Available: <http://www.sciencedirect.com/science/article/pii/S0169260712002829>
- [6] S. M. Kwok, R. Chandrasekhar, Y. Attikiouzel, and M. Rickard, "Automatic pectoral muscle segmentation on mediolateral oblique view mammograms," *Medical Imaging, IEEE Transactions on*, vol. 23, no. 9, pp. 1129–1140, 2004.
- [7] R. Ferrari, R. Rangayyan, J. E. L. Desautels, R. A. Borges, and A. Frere, "Automatic identification of the pectoral muscle in mammograms," *Medical Imaging, IEEE Transactions on*, vol. 23, no. 2, pp. 232–245, 2004.
- [8] Y. Li, H. Chen, Y. Yang, and N. Yang, "Pectoral muscle segmentation in mammograms based on homogenous texture and intensity deviation," *Pattern Recognition*, vol. 46, no. 3, pp. 681–691, 2013. [Online]. Available: <http://www.sciencedirect.com/science/article/pii/S003132031200427X>
- [9] F. Ma, M. Bajger, J. P. Slavotinek, and M. J. Bottema, "Two graph theory based methods for identifying the pectoral muscle in mammograms," *Pattern Recognition*, vol. 40, no. 9, pp. 2592–2602, 2007. [Online]. Available: <http://www.sciencedirect.com/science/article/pii/S003132030600522X>
- [10] C.-C. Liu, C.-Y. Tsai, J. Liu, C.-Y. Yu, and S.-S. Yu, "A pectoral muscle segmentation algorithm for digital mammograms using otsu thresholding and multiple regression analysis," *Computers & Mathematics with Applications*, vol. 64, no. 5, pp. 1100–1107, 2012. [Online]. Available: <http://www.sciencedirect.com/science/article/pii/S0898122112002337>
- [11] M. Mustra and M. Grgic, "Robust automatic breast and pectoral muscle segmentation from scanned mammograms," *Signal Processing*, vol. 93, no. 10, pp. 2817–2827, 2013. [Online]. Available: <http://www.sciencedirect.com/science/article/pii/S0165168412002563>
- [12] B.-W. Hong and B.-S. Sohn, "Segmentation of regions of interest in mammograms in a topographic approach," *Information Technology in Biomedicine, IEEE Transactions on*, vol. 14, no. 1, pp. 129–139, 2010.
- [13] S. Chatzistergos, I. Andreadis, and K. Nikita, "Tensor radial lengths for mammographic image enhancement," in *XIII Mediterranean Conference on Medical and Biological Engineering and Computing 2013*, ser. IFMBE Proceedings, L. M. Roa Romero, Ed. Springer International Publishing, 2014, vol. 41, pp. 305–308. [Online]. Available: http://dx.doi.org/10.1007/978-3-319-00846-2_76